Customization of Conductive Elastomer Based on PVA/PEI for Stretchable Sensors

Chan Wang, Kuan Hu, Chaochao Zhao, Yang Zou, Ying Liu, Xuecheng Qu, Dongjie Jiang, Zhe Li, Ming-Rong Zhang, and Zhou Li*

Conductive, stretchable, environmentally-friendly, and strain-sensitive elastomers are attracting immense research interest because of their potential applications in various areas, such as human–machine interfaces, healthcare monitoring, and soft robots. Herein, a binary networked elastomer is reported based on a composite hydrogel of polyvinyl alcohol (PVA) and polyethyleneimine (PEI), which is demonstrated to be ultrastretchable, mechanically robust, biosafe, and antibacterial. The mechanical stretchability and toughness of the hydrogels are optimized by tuning the constituent ratio and water content. The optimal hydrogel (PVA$_2$PEI$_1$-75) displays an impressive tensile strain as high as 500% with a corresponding tensile stress of 0.6 MPa. Furthermore, the hydrogel elastomer is utilized to fabricate piezoresistive sensors. The as-made strain sensor displays seductive capability to monitor and distinguish multifarious human motions with high accuracy and sensitivity, like facial expressions and vocal signals. Therefore, the elastomer reported in this study holds great potential for sensing applications in the era of the Internet of Things (IoTs).

The increasing demand for intelligent devices has risen exponentially in recent years, and the development of elastomers that are stretchable, flexible, and human-friendly has significance to meet the escalating requirements of increasing complexity and multifunctionality of modern electronics.[1,2] Devices such as epidermal electronics, implantable sensors,[3]

C. Wang, Dr. C. Zhao, Y. Zou, Y. Liu, X. Qu, D. Jiang, Z. Li, Prof. Z. Li
CAS Center for Excellence in Nanoscience
Beijing Key Laboratory of Micro-nano Energy and Sensor
Beijing Institute of Nanoenergy and Nanosystems
Chinese Academy of Sciences
Beijing 100083, China
E-mail: zli@binn.cas.cn
C. Wang, Dr. C. Zhao, Y. Zou, Y. Liu, X. Qu, D. Jiang, Z. Li, Prof. Z. Li
School of Nanoscience and Technology
University of Chinese Academy of Sciences
Beijing 100049, China
Dr. K. Hu, Prof. M.-R. Zhang
Department of Advanced Nuclear Medicine Sciences
National Institute of Radiological Sciences
National Institutes for Quantum and Radiological Science and Technology
263-8555 Chiba, Japan

The ORCID identification number(s) for the author(s) of this article can be found under https://doi.org/10.1002/smll.201904758.

point-of-care testing, and wearable energy devices[4] rely on intimate contact between devices and curvilinear surfaces of various biological systems while stably operating under up to 100% strain. Previously reported strategies for improving the performance of stretchable electronics majorly stemmed from strain engineering and nanocomposite approaches.[5] However, these methods show limitations in the next generation electronics, due to insufficient stretchability and sensitivity. Because of this, synthetical conductive elastomers with good stretchability and robustness have been intensely studied recently.[6,7]

Hydrogels are a class of viscoelastic materials with 3D networks and are able to absorb and retain a large amount of water.[8] Hydrogels are commonly composed of chemically or physically cross-linked hydrophilic polymers. The gelation of polymeric hydrogels is involved in a variety of mechanisms, including physical entanglement of polymer chains, electrostatic interactions, hydrogen bonds, and dynamic covalent chemical bonds.[9] The inherent water-abundant nature of hydrogels renders them broad applications in many fields, for examples, tissue engineering,[10] drug delivery,[10] soft electronics,[11–13] and actuators. However, most of the hydrogels are easy to be permanently broken because of limited mechanical strength. The broadened applications of hydrogels bring new requirements associated to mechanical parameters and physical configurations, such as introduction of active moieties in the hydrogels or tailoring of multiscale structures and architectures.[8] To implement these goals, several approaches such as rational design at the molecular level and control over multiscale architecture have been used to improve the mechanical properties of hydrogels.[2,5,14–17] For example, hydrogel formulations combined permanent polymer networks with reversible bonding chains for energy dissipation display strong toughness and stretchability.[14,15,18] Moreover, shear-thinning hydrogels that enrich reversible bonds impart a fluidic nature upon application of shear forces and return back to gel states once the forces are released. These advancements have rendered the hydrogels with wide applications in wearable electronics, soft robotics, and prosthetics.[11,15,19]

Harnessing hydrogel elastomers in wearable electronics has great significance and application prospects. To fabricate elastic hydrogels, researchers have tried to introduce self-healing

**ADVANCED
SCIENCE NEWS**
www.advancedsciencenews.com

NANO · MICRO
small
www.small-journal.com

Table 1. Summary of the reports about PVA/PEI-based composition and their antibacterial properties, recent years.

Component	Mechanism	Method	Form	Application	Refs.
PVA/oxCNTs@QPEI	–	Solvent casting	Film	Antibacterial	[21]
PVA/rGO/PEI	Hydrogen bond	One-pot strategy	Film	Strength and toughness improvement	[24a]
Glycidyl methacrylate modified PVA/PEI (a-PVA/a-PEI)	–	Electrospinning and in situ photo crosslinking	Nanofiber membranes	Virus clearance tests	[25]
PVA/PEI/PCL	Hydrogen bond	Electrospinning	Composite membrane	Drug-delivery carriers or tissue-engineering scaffolds	[24b]
PVA—PEI	Formation of —CN— groups	In situ crosslink	–	Polymer binder for Li-ion batteries	[23]
(PVA/PEI)/AgNPs	–	Electrospinning	Nanofibre hybrids	Antibacterial	[26]
(PVA/PEI)/AgNPs	–	In situ reduction / electrospinning	Nanofibers	H_2O_2, glutathione (GSH) and glucose detection biosensor	[22]

moieties or electrostatic pairs in engineering hydrogels. By doing this, the mechanical properties of the hydrogels were significantly improved. However, the polymers with complex functionalities and complicated structures were difficult to synthesize and increase the production expenses.[14,16,20,21] Besides, polymers with complicated structures show limitations of large-scale industrial production, thus impedes practical applications. In this context, the development of elastic hydrogels that are cost-effective, easy synthesis, and atom economy are desperately needed. Aim to facilely synthesize elastic hydrogels with readily accessible materials, we paid attention to commercialized and cheap polymers, such as polyvinyl alcohol (PVA) and chitosan. Based on these polymers, we synthesized 8 kinds of hydrogels and evaluated their mechanical properties (Table S1, Supporting Information). Among them, a hydrogel composed of PVA and polyethyleneimine (PEI) showed the best stretchability.

The PVA/PEI copolymer has been widely used in antibacterial materials,[22] biosensors,[23] drug delivery vehicles,[8,10] and a binder of Li-ion battery,[24] as summarized in **Table 1**.[22,23,25–27] These studies revealed that the PVA/PEI copolymer is biocompatible and stretchable. Together with our findings, we conceived that the PVA/PEI copolymers would be potential materials for elastomer, and the mechanical properties of the hydrogel elastomer can be tuned by varying the constituent and optimizing the processing methods, since PVA and PEI show opposite charges in solution.

Herein, we developed a stretchable elastomer based on a composite hydrogel of PVA and PEI, which shows excellent biocompatibility and remarkable mechanical properties. The elastomer was synthesized by a solution–gel method coordinated with a freezing/thawing process.[6,28] Briefly, PVA and PEI were dissolved in deionized water and heated by a water bath to form a homogeneous solution. Then the viscous solution transformed into elastomer through a freezing/thawing process. In this binary system, multiple interactions between PVA and PEI, as well as the interactions between polymers and water molecules, provide the molecular basis of elasticity. First, the entanglements of the polymer chains due to the electrostatic interactions serve as cross-linking points and stress transfer centers. Second, the intramolecular hydrogen bonds in PEI or PVA, and intermolecular hydrogen bonds between the hydroxyl

group (—OH) and the amino group (NH—) afford dynamic exchange points during the stretching and releasing cycles. The breaking of hydrogen bonds can dynamically recombine to dissipate energy and homogenize the network under stretching.[14] **Figure 1**a shows a conceptual diagram of the elastomer (left). The chemical formulations and hypothesized hydrogen bond networks are illustrated (Figure 1a, middle). The Figure 1a (right) is the optical images of the elastomer, which is semi-transparent and stretchable.

The mechanical properties of hydrogel are majorly determined by several parameters, e.g., constituent ratio, water content, and processing methods.[1,8] In particular, by subtle tuning of constituent ratio, the assembly modes of the polymers in the hydrogels would significantly vary, thus leads to dramatical improvement of mechanical properties of the hydrogels. On this basis and aim to maximize the mechanical properties, we synthesized hydrogels with different ratios of PVA and PEI and tested the stretchability. As shown in Figure 1b, the tensile strength and strain display linear correlation, in accordance with Hooke's law. These results indicate good elasticity of the hydrogels. The Young's modulus and breaking length of PVA_2PEI_1 (the subscript means the mass ratio of the polymer, similarly hereinafter), PVA_1PEI_1, and PVA_1PEI_2 were calculated and summarized in Figure 1c. The tensile strength and breaking elongation of the elastomers increased with the increasing of content of PVA. For PVA_2PEI_1, its breaking strain reached 500% of the original length, with a tensile stress approaches 600 kPa, which are two folds and six folds of that of PVA_1PEI_2, respectively. The stronger tensile stress is probably caused by the more intense entanglement of the polymer chains of PVA due to the larger molecular weight. Moreover, the hydroxyl groups in PVA are good hydrogen bond donors which may attribute to stronger hydrogen bond networks.

To further explore the effect of constituent content, Fourier-transform infrared spectroscopy (FTIR) was performed. As shown in Figure S1a (Supporting Information), the broad peak spanning from 3380 to 3250 cm^{-1} and the weak peak around 1100 cm^{-1} are attributed to v—OH stretching of PVA. Similarly, v—R_2NH stretching of PEI could be assigned to the broad peak (dash area) at 1042 cm^{-1}. The peak intensity from v—OH showed a downtrend along with the increase of PEI in elastomer, contrary to v—R_2NH's.[24–26] Furthermore, we performed
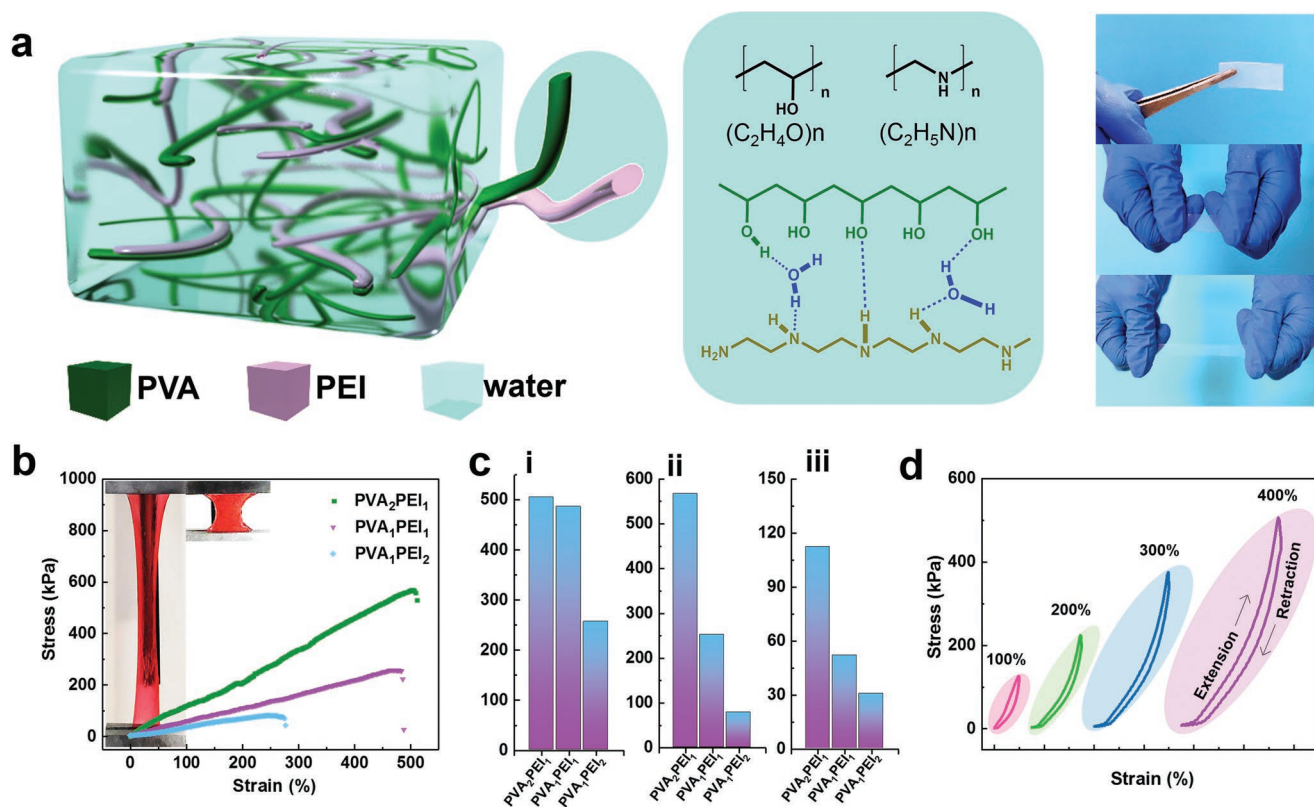
Figure 1. Concept illustration and mechanical properties of the elastomer based on PVA/PEI hydrogel. a) Concept diagram, molecular structure, and optical images of the elastomer. b) Stress–strain curves of the hydrogel with different ratio of PVA to PEI (by mass). The 2 and 1 respect to the proportion of PVA and PEI in PVA_2PEI_1, the water content of the elastomer was 75%. The inset of (b) shows a sample with a dimension of 15 mm in length, 10 mm in width, and 2 mm in thickness without stretch (right) and while stretched to 400% (left). c) Histograms show elongation at break (%) (I), tensile strength (kPa) (II), and Young's modulus (kPa) (III) of the elastomers named PVA_2PEI_1, PVA_1PEI_1, and PVA_1PEI_2. d) Sequential extension–retraction cycle curves without rest intervals, when the elastomer (PVA_2PEI_1) was stretched to 100%, 200%, 300%, and 400%.

X-ray Diffraction (XRD) (Figure S1b, Supporting Information) to study the elastomer's crystallization behavior. More PVA in elastomer helps to form crystallization at some local areas. This phenomenon is most likely to cause by the ordered molecular organization of the polymer in the hydrogels.[25] To examine the recoverability of the elastomer after stretching (Figure 1d), the loading–unloading cycle test was performed. Obviously, energy dissipation for strain is manifested as prominent hysteresis loops beyond the linear regime. When the applied tensile strain was 100%, the elastomer can completely recover to the original state. However, when deformation increased to 200%, the material can be restored to a stretch of 25%, indicating occurrence of irreversible deformation. When the stretch deformation increases to 300% or 400%, the irreversible deformation amplified to be near 50% of its original state. The excellent recoverability under 100% tensile strain renders them great potential in wearable devices, e.g., pressure sensors.

The water content is another vital parameter to determine the mechanical property of the elastomer. The influence of water content in the PVA/PEI system was investigated. As shown in the conceptual diagram in **Figure 2**a, the water molecules filled and buried in the polymer framework, and are either bound to the polar polymers to mitigate the spatial hindrance between the polymer chains or just behaved as free water. The stress–strain curves of elastomers with different water content (75%,

80%, and 85% by mass) were tested (Figure 2b). The breaking elongation, tensile strength, and Young's modulus decreased with the increase of water content (more details in Figure S2, Supporting Information). Increasing the water content from 75% to 85%, both the strain and strength of the hydrogel significantly declined, as about 30% of the tensile strain and 10% of the stress retained. The huge differences may be related to the status of water molecules in the hydrogels. Plethora of free water molecules (without hydrogen bonding formation) in the system would weaken the dynamic hydrogen bonding interactions between the polymers. The water contents in the elastomer were further confirmed by thermogravimetric analysis (TGA; Figure S3, Supporting Information). The critical temperature point (the end of water evaporation) of PVA_2PEI_1-75/80/85 occurred to be 156/151/127 °C, respectively. These temperatures are much higher than the boiling temperature of water. Besides, slight differences in moisture evaporation temperatures of the three kinds of hydrogels, indicating different bonding status of the water molecules in the systems.[29]

To study the stability and durability of the elastomer in atmosphere, we placed the hydrogel PVA_2PEI_1-80 in a Petri dish and measured changes in water content as well as their mechanical properties for one month. The water evaporated quickly from the hydrogel at the first week, then gradually slowed down, and
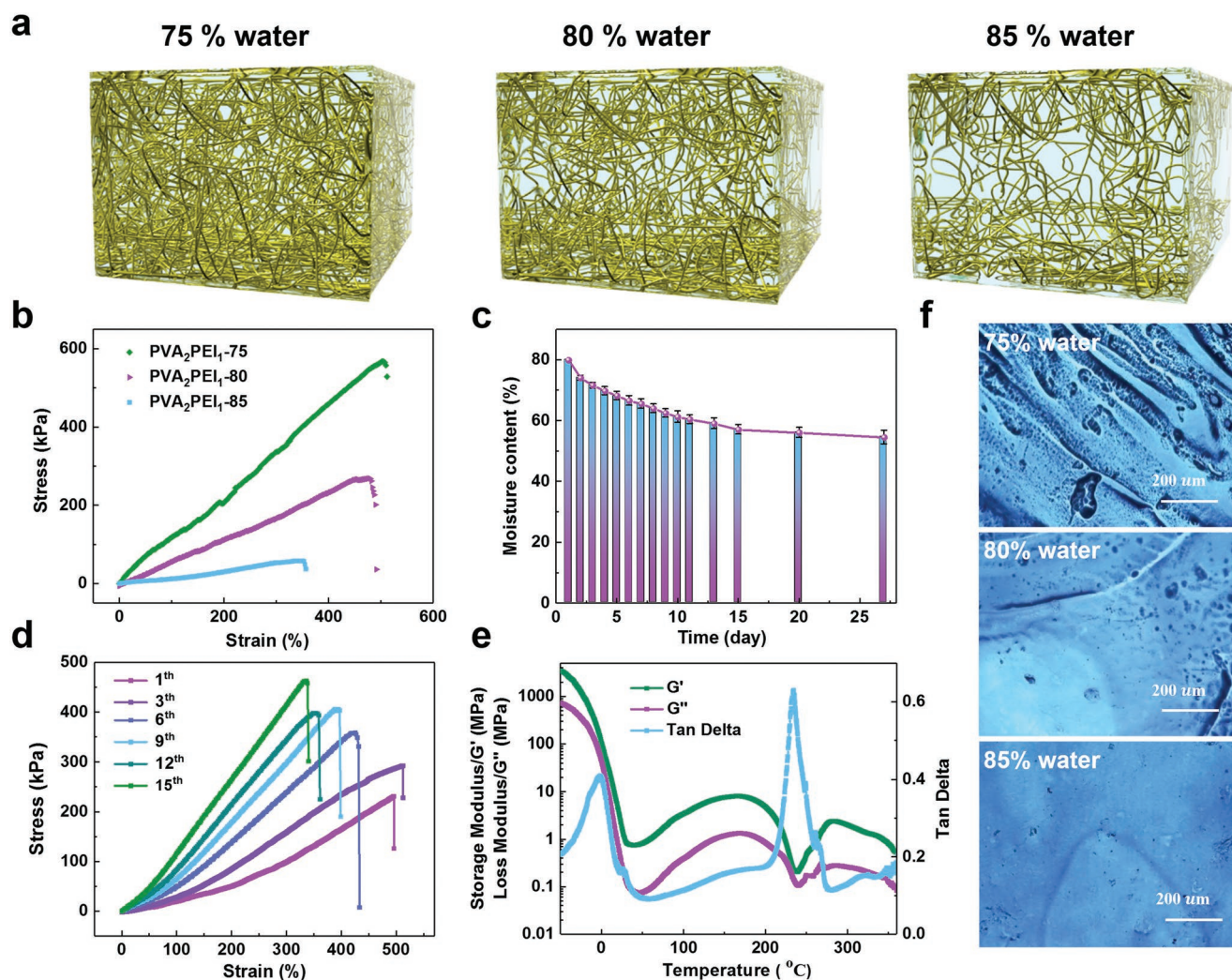
Figure 2. Research on properties of the elastomer (PVA/PEI is 2:1 by mass) with different water contents. a) Concept diagram of the hydrogel with 75%, 80%, and 85% water content. b) Stress–strain curves and f) optical images of the hydrogel with different water content. Scale bar 200 um. c) The water content of the hydrogel left in air varies with the days and the initial water content is 80% by mass. d) Stress–strain curves of the hydrogel exposed in air for different days. e) Storage Modulus (G′) and Loss Modulus (G″) for the hydrogel (PVA$_2$PEI$_1$-75). The Tan Delta was calculated based on reference.

finally stabilized at around 60% (Figure 2c). The mechanical properties of the elastomers were recorded in different placing days, as shown in Figure 2d. As the water content decreases, the maximum stretchable length of the material decreases while Young's modulus increases oppositely. The losing of water molecules enhances the direct interpolymer interactions, while weakens the solvation effects in the hydrogels. As a result, the free slipping of the polymer chains became difficult, resulting in an increase in Young's modulus.[16] The optical photographs of the elastomer (Figure 2f) with different water contents also reflected the phenomenon. When the water content is 75%, obvious wrinkles were exhibited on the surface of the hydrogel, however, the wrinkle disappeared when the water content is 85%, replacing with flat and smooth surface of the elastomer. Furthermore, the PVA$_2$PEI$_1$-75 was chosen to take temperature-dependent mechanical properties analysis (DMA). As shown in Figure 2e, the Storage Modulus (G′) is much higher than Loss Modulus (G″) from −5 to 360 °C, indicating superior elasticity

and strength. There are two transitions observed in the tan δ plot at −2 °C and 234 °C during heating. We attributed the first thermal transition to the breaking of hydrogen bonds between side chain groups, like the interactions between hydroxyl and amino groups. The second transition point confirmed to be glass transition, which may be caused by the breaking of the polymer chains.[21,30] The DMA of the elastomers suggests good elasticity in the normal temperature range, making them as promising material for flexible electronic devices.

Having demonstrated the excellent mechanical properties of the PVA/PEI elastomer, we further investigated the electrical conductivity of the hydrogel, as the electrical conductivity is critical for fabricating wearable electronics. In the PVA/PEI hydrogel system, the conductivity majorly originated from the proton flow, however, this kind of conductivity is prone to the environmental conditions. Adding lithium chloride (LiCl) in hydrogels is a widely adopted strategy to improve the conductivity, since the Li$^+$ is the smallest metallic ions with high

ADVANCED
SCIENCE NEWS
www.advancedsciencenews.com
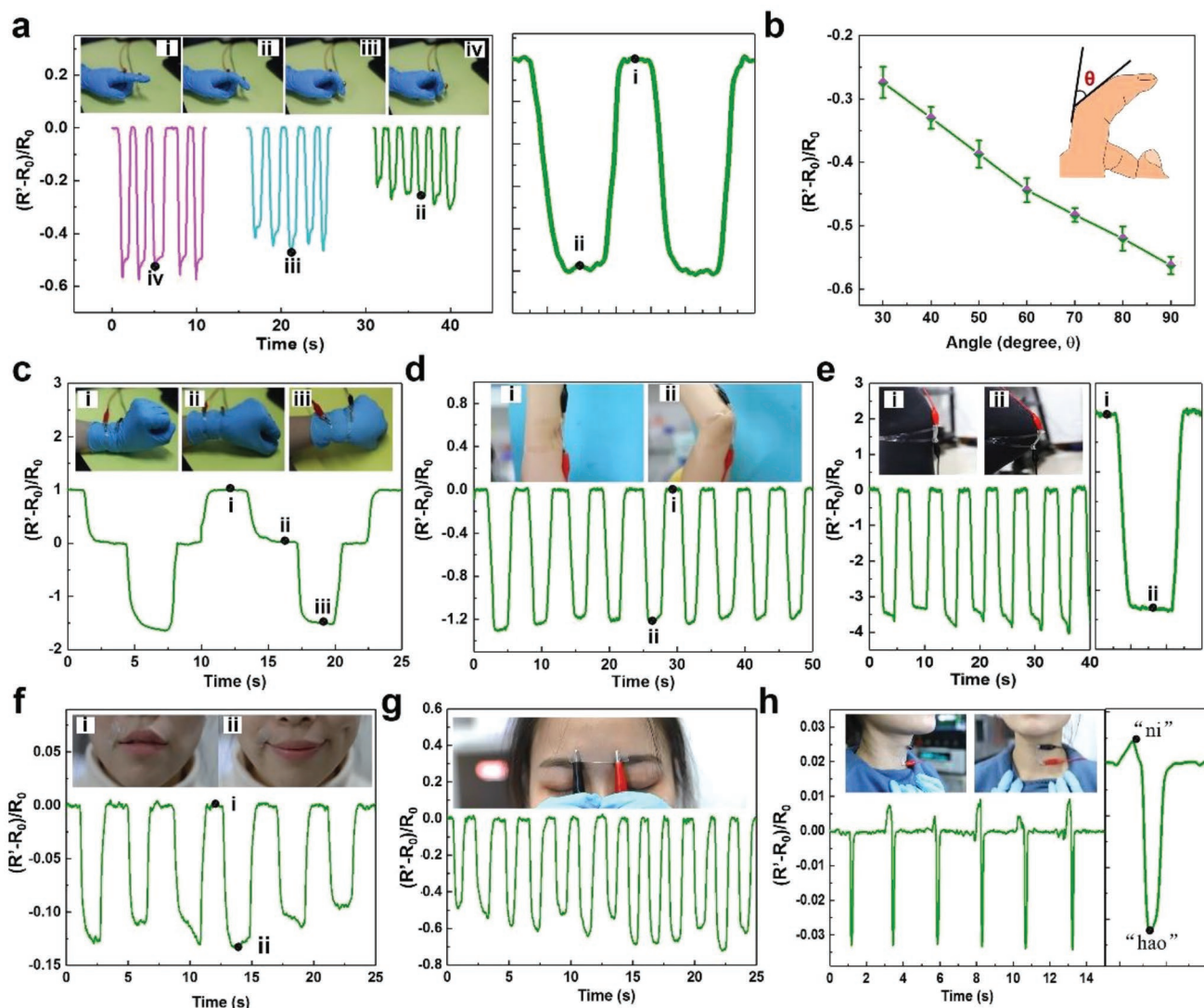
NANO · MICRO
small
www.small-journal.com
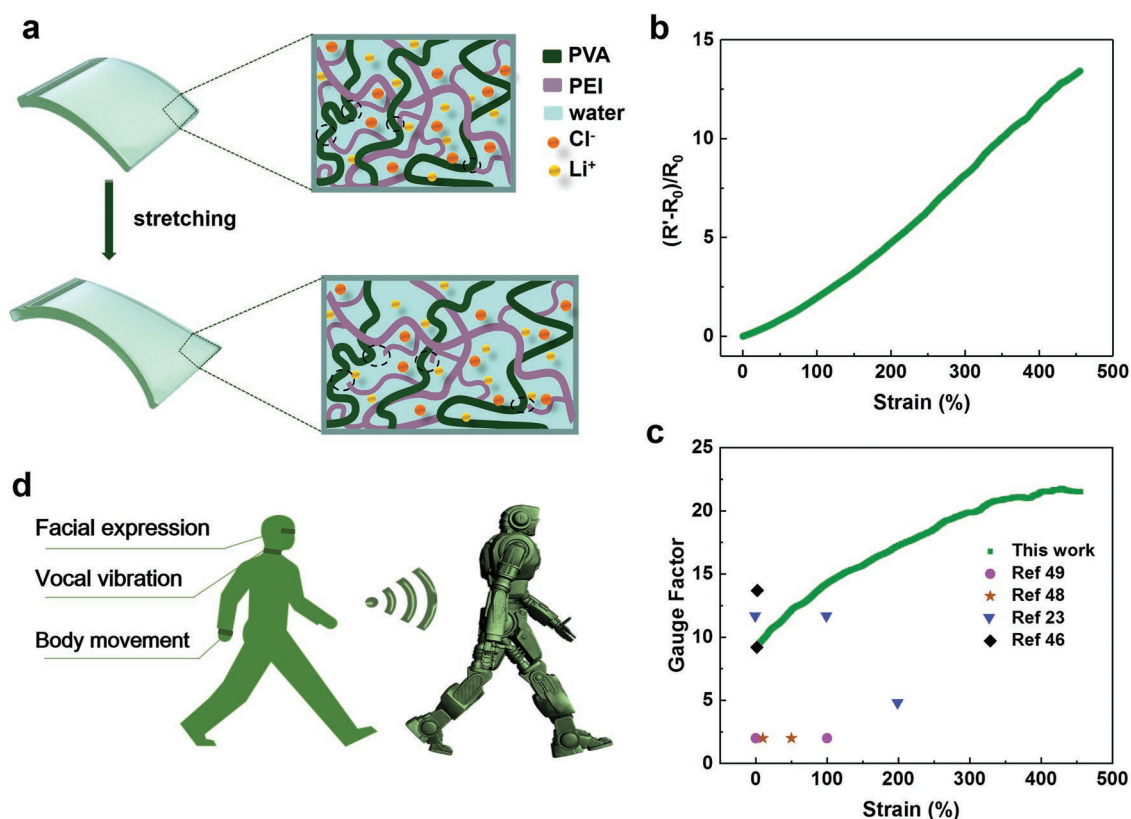
Figure 3. Applications of the stretchable elastomer for piezoresistive sensors for human motion monitoring. a) Concept diagram of the elastomer used as sensor in original and stretchable state. The inset schematic showing the mechanism of the resistance changing along with the hydrogel stretched. b) The resistance changed along with strain. c) Gauge factors measured as a function of applied strain. d) Schematic illustration of the sensor attached to different parts for detecting subtle human motions and can be used in commanding robot in the future.

stability in different conditions.[10,12,30] A ternary hydrogel system, named PVA_2PEI_1-LiCl, was prepared, in which the concentration of LiCl is about 4 mol L^{-1}. The ternary system possesses several advantages. First, the mechanical strength of the hydrogel was enhanced because of the strong ion–polymer interactions (Figure S4, Supporting Information). Second, the conductivity of the hydrogel was dramatically improved, given that the Li^+ ions and Cl- ions could harmoniously shuttle in the hydrogel. The hydrogen bond networks in the hydrogel provide conductive pathways for ion transport (Li^+ and Cl^-).[31] (**Figure 3**a). So far, the PVA_2PEI_1-LiCl hydrogel fulfills most of the conditions for fabricating wearable sensors. Hence, a piezoresistive sensor with a size of $2 \times 1 \times 0.2$ cm^3 was fabricated. The correlation between the resistance variations and the tensile strain was tested. As shown in Figure 3b, with the tensile strain increased, the resistance of the sensor gradually increased from the 730 ohms to ≈10 000 ohms at 4.5-fold stretch. Then we calculated the Gauge Factor (GF) of the elastomer under different stretch state. The GF is defined as the ratio of relative change in electrical resistance R to the mechanical strain ε, and is expressed as GF = $((R - R_o)/R_o)/\varepsilon)$.[32] The GFs is an indicator of the sensitivity of the sensor, where the value is bigger, the sensor is more sensitive to strain. The GF for the PVA_2PEI_1-LiCl sensor is 9 at 0% strain, and is sharply increased as the strain reached 450%, where the GF is near 22. These values are greater than many of the previously reported

similar sensors.[14,33] Besides, the sensor displays superior stability, it can stably operate up to 6000 cycles (Figure S5, Supporting Information). To sum up, the PVA_2PEI_1-LiCl is an excellent material for fabricating piezoresistive sensors to detect human motions, including body movements, facial expressions, or even vocal vibrations. By doing this, the sensor is expected to have diverse applications in the era of the IoTs, such as human real-time remote control of the robot for task implementation (Figure 3d).

Due to the outstanding mechanical profile, wide working range, sticky and innocuous to the human body, the piezoresistive sensor can be readily adhered to various positions on the human body with complex 3D geometry without adhesives to detect various bodily motions. For demonstration, the elastomer was shaped into different sizes to adapt different surfaces of the body, such as the finger, wrist, elbow, knee, corners of the mouth, neck, and glabellum. As shown in **Figure 4**a, the sensor was mounted on the index finger to monitor the bending state. The relative resistance change is uniform when the finger bent at a certain angle (i) initial; ii) 30°; iii) 60°; iv) 90°), and the angles of the finger bending could be precisely tracked by monitoring the relative change in resistance, revealing by the linear correlation between the changes of the resistance and the bending angles (Figure 4b). Moreover, the signal was clear and stable under different states. The motion state of the wrist could also be monitored through changes in the resistance of

ADVANCED
SCIENCE NEWS
www.advancedsciencenews.com

NANO · MICRO
small
www.small-journal.com

Figure 4. Applications of the stretchable elastomer for piezoresistive sensors for human motion monitoring. a) Relative resistance changes when fingers at different bending angles: i) original state; ii) bending at 30°; iii) bending at 60°; iv) bending at 90°. The inset shows two pulses during the finger was in original and 30° state. b) Relative resistance and bending angles show a liner relationship. c) The resistance changed during bending wrist: i) bending up; ii) original state; iii) bending down. d) The resistance changed during bending arm: i) original state; ii) bending state. e) The resistance changed during bending leg. The right inset shows single pulse of i) original state and ii) bending state. f) Relative resistance changes: i) deadpan and ii) smiling. g) The resistance changed during frowning. h) Relative resistance changes when the volunteer say "ni hao" (hello). The right inset shows a single pulse of i) "ni" and ii) "hao".

the sensor, (i)bending up; ii) original state; iii) bending down), as shown in Figure 4c. Similarly, we also attached the sensor to elbow (Figure 4d) and knee (Figure 4e) to monitor its response toward the movement of the joint. Besides, the piezoresistive sensor could also be used to monitor more complex signals or gestures from subtle human movements, such as facial expressions and pronunciation. The strain sensor was adhered to the mouth corner to detect facial expressions of i) deadpan and ii) smiling, and the plots of relative resistance change versus time for deadpan and smiling are depicted in Figure 4f, which delicate peak-valley waveforms allow for accurate facial expression monitoring. When adhering to the middle of the forehead, the frowning can be distinguished as the resistance changed.

The above tests have revealed the unique capabilities of the sensor to detect tiny human motions, therefore, more advanced sensing, such as detecting another vital signal that urgently demands precise monitoring, namely the phonatory process (voicing), was performed. The strain sensor was attached at the throat for recognizing the muscle motion induced by speaking "ni hao" (你好, hello), and signals with the words are demonstrated in Figure 4h. The above results indicate the excellent performance of the strain sensors for detecting human motions.

To further investigate the biocompatibility of the as-prepared elastomer, the cytotoxicity of PVA/PEI hydrogel was evaluated by in vitro coculture with L929 cells (see Experimental Methods Section in the Supporting Information).[35] Cells seeded without
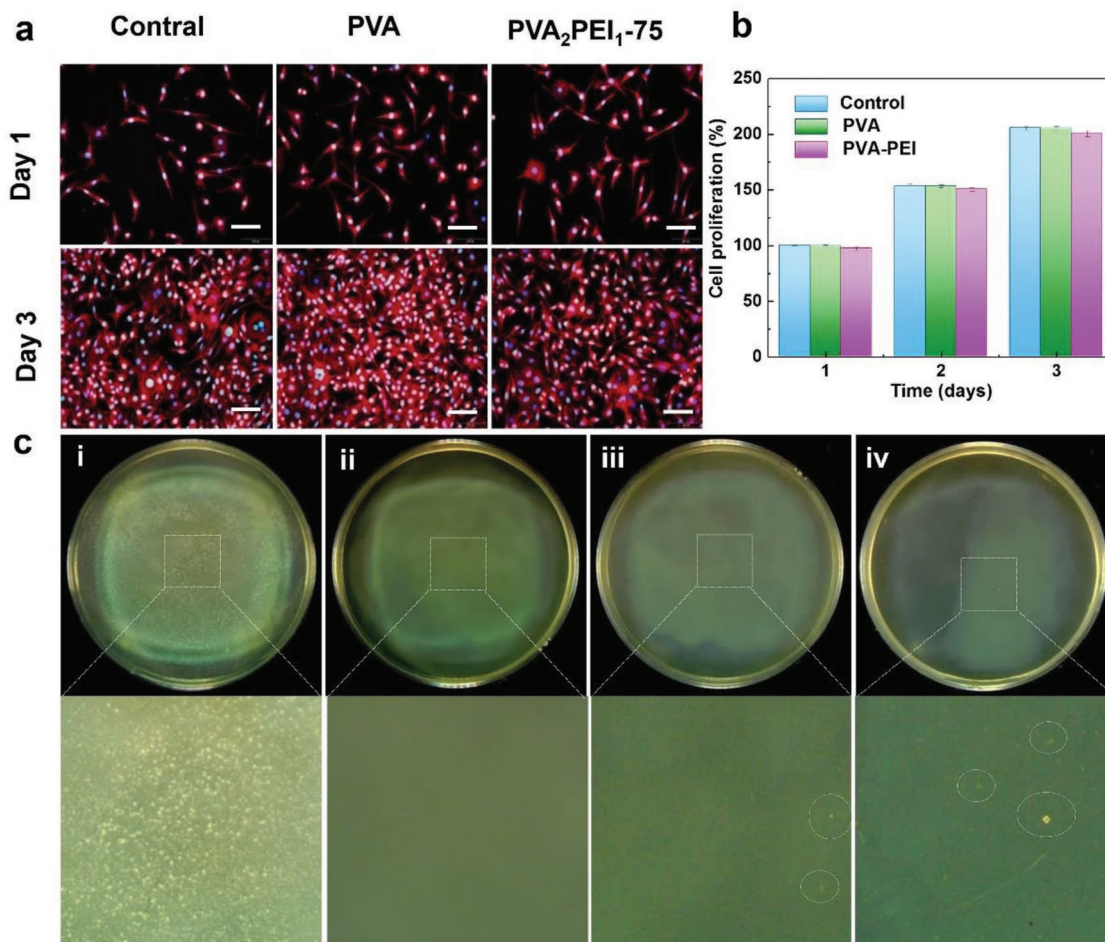
Figure 5. Characterization of biocompatibility and antimicrobial properties of the hydrogel. a) Biocompatibility of constituent materials of blank, PVA, and PVA$_2$PEI$_1$-75. Attachment, proliferation, and morphology of the L929 cells at different time. Scale bars: 100 µm. b) Cell viability of constituent materials assessed by MTT assay for 1, 2, 3 d. c) Photographs of *E. coli* after coculturing for 18 h with the composite samples: i) blank; ii) PEI; iii) PVA$_2$PEI$_1$-75; iv) PVA-Ag.

sample extracts were used as control. Representative fluorescence images are shown in **Figure 5**a and Figure S6 (Supporting Information). After culture for 1 d, similar live cell (red) densities were observed for all the groups, indicating none cytotoxicity of the samples.[36] Later, cells continuously proliferated and spread homogeneously until full coverage after 3 d of culture, indicating good cell proliferation of the elastomer treated cells. The 3-(3-(4,5-dimethyl-2-thiazolyl)-2,5-diphenyl-2-H-tetrazolium bromide (MTT) assay was used to quantitative measurement of cell viability after treatments. As shown in Figure 5b, the cells in different groups (control, PVA, and PVA$_2$PEI$_1$-75) for 1, 2, and 3 d treatments show almost the same cell viabilities, confirming good biocompatibility of PVA$_2$PEI$_1$ hydrogel. These results are consistent with the results in Figure 5a. After that, the antibacterial properties of the materials were examined. Escherichia coli (*E. coli*) was used to test the antibacterial effect of the elastomer in a fluid nutrient medium. As shown in Figure 5c, the experimental groups (PEI, PVA$_2$PEI$_1$-75, PVA/Ag) showed almost no survived *E. coli* after coculture for 18 h at 37 °C compared with blank. Table S2 (Supporting Information) shows the antibacterial efficiency of the samples. The PVA-PEI elastomer shows comparable antibacterial

property with PVA-Ag$^+$, which was reported to be excellent bactericidal materials previously.[37] These results all suggest that the PVA-PEI hydrogels are biocompatible and antibacterial.

In summary, we developed an ultrastretchable elastomer based on PVA/PEI hydrogel, which is durable, adhesive, sensitive, biosafety and antimicrobial. We investigated the influence of constituent ratio and water content on the performance of the mechanical properties of the elastomer. The optimal hydrogel is opted to be PVA$_2$PEI$_1$-75, which displays a tensile strain as high as 500% with a corresponding tensile stress of 0.6 MPa, featuring a durable working time for more than 3 weeks. These studies help to rational design of novel materials and strengthen the understanding of molecular interactions in the hydrogels. We further fabricated piezoresistive sensors by utilizing the binary hydrogels. The as-prepared strain sensor showed seductive potency to monitor and distinguish multifarious human motion with high accuracy and sensitivity, like facial expressions and vocal signals. The unique sensing capability demonstrated in this work can be extended to other more complicated sensing applications that involve 3D motions, including touch sensing and biosignal monitoring. To

ADVANCED
SCIENCE NEWS

www.advancedsciencenews.com

NANO · MICRO
small
www.small-journal.com

conclude, we have designed a cost-effective, robust, and ultrastretchable hydrogel system based on PVA and PEI, which is a promising material platform for various applications in the era of IoTs.

Supporting Information

Supporting Information is available from the Wiley Online Library or from the author.

Conflict of Interest

The authors declare no conflict of interest.

[1] J. F. Patrick, M. J. Robb, N. R. Sottos, J. S. Moore, S. R. White, *Nature* **2016**, *540*, 363.

[2] a) X. H. Z. Li, H. Zhang, P. Zhang, Y. Yu, *Chem. Mater.* **2018**, *30*, 3752; b) Z. X. Deng, Y. Guo, X. Zhao, P. X. Ma, B. L. Guo, *Chem. Mater.* **2018**, *30*, 1729.

[3] a) H. Ouyang, J. J. Tian, G. L. Sun, Y. Zou, Z. Liu, H. Li, L. M. Zhao, B. J. Shi, Y. B. Fan, Y. F. Fan, Z. L. Wang, Z. Li, *Adv. Mater.* **2017**, *29*, 1703456; b) Y. D. Cao, T. Li, Y. Gu, H. Luo, S. Q. Wang, T. Zhang, *Small* **2018**, *14*, 1703902; c) Q. Wang, M. Q. Jian, C. Y. Wang, Y. Y. Zhang, *Adv. Funct. Mater.* **2017**, *27*, 1605657.

[4] a) C. Wang, K. Hu, W. J. Li, H. Y. Wang, H. Li, Y. Zou, C. C. Zhao, Z. Li, M. Yu, P. C. Tan, Z. Li, *ACS Appl. Mater. Interfaces* **2018**, *10*, 34302; b) H. Li, C. C. Zhao, X. X. Wang, J. P. Meng, Y. Zou, S. Noreen, L. M. Zhao, Z. Liu, H. Ouyang, P. C. Tan, M. Yu, Y. B. Fan, Z. L. Wang, Z. Li, *Adv. Sci.* **2019**, *6*, 1801625; c) S. Gong, W. Cheng, *Adv. Energy Mater.* **2017**, *7*, 1700648; d) X. Q. Liao, Z. Zhang, Z. Kang, F. F. Gao, Q. L. Liao, Y. Zhang, *Mater. Horiz.* **2017**, *4*, 502.

[5] D. H. Kim, J. Z. Song, W. M. Choi, H. S. Kim, R. H. Kim, Z. J. Liu, Y. Y. Huang, K. C. Hwang, Y. W. Zhang, J. A. Rogers, *Proc. Natl. Acad. Sci. USA* **2008**, *105*, 18677.

[6] H. J. Zhang, H. S. Xia, Y. Zhao, *ACS Macro Lett.* **2012**, *1*, 1233.

[7] a) C. Wang, K. Xia, H. Wang, X. Liang, Z. Yin, Y. Zhang, *Adv. Mater.* **2019**, *31*, 1801072; b) M. Amit, L. Chukoskie,

[8] H. Yuk, B. Y. Lu, X. H. Zhao, *Chem. Soc. Rev.* **2019**, *48*, 1642.

[9] J. Chen, Q. C. Dong, X. Y. Ma, T. H. Fan, Y. Lei, *Sci. Rep.* **2016**, *6*, 30804.

[10] S. Merino, C. Martín, K. Kostarelos, M. Prato, E. Vázquez, *ACS Nano* **2015**, *9*, 4686.

[11] Y. Wang, Ch. X. Zhu, R. Pfattner, H. P. Yan, L. H. Jin, S. C. Chen, F. Molina-Lopez, F. Lissel, J. Liu, N. I. Rabiah, Z. Chen, J. W. Chung, C. Linder, M. F. Toney, B. Murmann, Z. N. Bao, *Sci. Adv.* **2017**, *3*, e1602076.

[12] a) C. Tondera, T. F. Akbar, A. K. Thomas, W. L. Lin, C. Werner, V. Busskamp, Y. X. Zhang, I. R. Minev, *Small* **2019**, *15*, 1901406; b) B. C. Tee, C. Wang, R. Allen, Z. N. Bao, *Nat. Nanotechnol.* **2012**, *7*, 825; c) N. Liu, A. Chortos, T. Lei, L. H. Jin, T. R. Kim, W. G. Bae, Ch. X. Zhu, S. H. Wang, R. Pfattner, X. Y. Chen, R. Sinclair, Z. N. Bao, *Sci. Adv.* **2017**, *3*, e1700159.

[13] L. Shi, T. X. Zhu, G. X. Gao, X. Y. Zhang, W. Wei, W. F. Liu, S. J. Ding, *Nat. Commun.* **2018**, *9*, 2630.

[14] Z. J. Wang, C. P. Xiang, X. Yao, P. L. Floch, J. Mendez, Z. G. Suo, *Proc. Natl. Acad. Sci. USA* **2019**, *116*, 5967.

[15] T. Wang, Y. Zhang, Q. C. Liu, W. Cheng, X. R. Wang, L. J. Pan, B. X. Xu, H. X. Xu, *Adv. Funct. Mater.* **2018**, *28*, 1705551.

[16] E. Filippidi, T. R. Cristiani, C. D. Eisenbach, J. H. Waite, J. N. Israelachvili, B. K. Ahn, M. T. Valentine1, *Science* **2017**, *358*, 502.

[17] Y. Z. Zhang, K. H. Lee, D. H. Anjum, R. Sougrat, Q. Jiang, H. Kim, H. N. Alshareef, *Sci. Adv.* **2018**, *4*, eaat0098.

[18] a) J. H. Kang, D. H. Son, G. J. N. Wang, Y. X. Liu, J. Lopez, Y. Kim, J. Y. Oh, T. Katsumata, J. Mun, Y. J. Lee, L. H. Jin, J. B. H. Tok, Z. N. Bao, *Adv. Mater.* **2018**, *30*, 1706846; b) Y. J. Jung, S. Kar, S. Talapatra, C. Soldano, G. Viswanathan, X. S. Li, Z. L. Yao, F. S. Ou, A. Avadhanula, R. Vajtai, S. Curran, O. Nalamasu, P. M. Ajayan, *Nano Lett.* **2006**, *6*, 413.

[19] a) M. A. Darabi, A. Khosrozadeh, R. Mbeleck, Y. Q. Liu, Q. Chang, J. Z. Jiang, J. Cai, Q. Wang, G. X. Luo, M. Xing, *Adv. Mater.* **2017**, *29*, 1700533; b) C. M. Boutry, Z. Wang, J. Chang, Y. Kaizawa, B. C. Schroeder, P. Fox, Z. N. Bao, *Nat. Electron.* **2018**, *1*, 314; c) Z. Y. Lei, P. Y. Wu, *Nat. Commun.* **2018**, *9*, 1134; d) J. Wu, Z. X. Wu, H. H. Xu, Q. Wu, C. Liu, B. R. Yang, X. C. Gui, X. Xie, L. K. Norforde, *Mater. Horiz.* **2019**, *6*, 595.

[20] S. Seo, D. W. Lee, J. S. Ahn, K. Cunha, E. Filippidi, S. W. Ju, E. Shin, B. S. Kim, Z. A. Levine, R. D. Lins, J. N. Israelachvili, J. H. Waite, M. T. Valentine, J. E. Shea, B. K. Ahn, *Adv. Mater.* **2017**, *29*, 1703026.

[21] J. C. Lai, L. Li, D. P. Wang, M. H. Zhang, S. R. Mo, X. Wang, K. Y. Zeng, Ch. H. Li, Q. Jiang, X. Z. You, . L. Zuo, *Nat. Commun.* **2018**, *9*, 2725.

[22] A. Sapalidis, Z. Sideratou, K. N. Panagiotaki, E. Sakellis, E. P. Kouvelos, S. Papageorgiou, F. Katsaros, *Front. Mater.* **2018**, *5*, 11.

[23] H. Zhu, M. L. Du, M. Zhang, P. Wang, S. Y. Bao, L. N. Wang, Y. Q. Fu, J. M. Yao, *Biosens. Bioelectron.* **2013**, *49*, 210.

[24] Z. Liu, S. Han, C. Xu, Y. W. Luo, N. Peng, C. Y. Qin, M. J. Zhou, W. Q. Wang, L. W. Chen, S. Okada, *RSC Adv.* **2016**, *6*, 68371.

[25] a) L. S. Shao, J. J. Li, Y. Guang, Y. L. Zhang, H. Zhang, X. Y. Che, Y. H. Wang, *Mater. Des.* **2016**, *99*, 235; b) C. H. Dong, X. Y. Yuan, M. Y. He, K. D. Yao, *J. Biomater. Sci., Polym. Ed.* **2006**, *17*, 631.

[26] B. Zeytuncu, M. Ürper, İ. Koyuncu, V. V. Tarabara, *Sep. Purif. Technol.* **2018**, *197*, 432.

[27] P. Wang, H. Zhu, S. Bao, M. L. Du, M. Zhang, *J. Phys. D: Appl. Phys.* **2013**, *46*, 345303.

[28] Y. M. Chen, W. Q. Qian, R. Chen, H. J. Zhang, X. J. Li, J. D. Shi, W. F. Dong, M. Q. Chen, Y. Zhao, *ACS Macro Lett.* **2017**, *6*, 1129.

[29] U. Habiba, T. A. Siddique, J. J. Li Lee, T. C. Joo, B. C. Ang, A. M. Afifi, *Carbohydr. Polym.* **2018**, *191*, 79.

[30] N. Oya, T. Ikezaki, N. Yoshie, *Polym. J.* **2013**, *45*, 955.

[31] B. W. Yang, W. Z. Yuan, *ACS Appl. Mater. Interfaces* **2019**, *11*, 16765.

[32] Y. Ding, J. J. Zhang, L. Chang, X. Q. Zhang, H. L. Liu, L. Jiang, *Adv. Mater.* **2017**, *29*, 1704253.

[33] a) E. Roh, B. U. Hwang, D. Kim, B. Y. Kim, N. E. Lee, *ACS Nano* **2015**, *9*, 6252; b) Z. Yang, Y. Pang, X. L. Han, Y. F. Yang, J. Ling, M. Q. Jian, Y. Y. Zhang, Y. Yang, T. L. Ren, *ACS Nano* **2018**, *12*, 9134.

[34] a) S. G. Yoon, H. J. Koo, S. T. Chang, *ACS Appl. Mater. Interfaces* **2015**, *7*, 27562; b) H. Y. Qiao, P. F. Qi, X. H. Zhang, L. N. Wang, Y. Q. Tan, Z. H. Luan, Y. Z. Xia, Y. H. Li, K. Y. Sui, *ACS Appl. Mater. Interfaces* **2019**, *11*, 7755.

[35] C. C. Zhao, H. Q. Feng, L. M. Zhang, Z. Li, Y. Zou, P. C. Tan, H. Ouyang, D. J. Jiang, M. Yu, C. Wang, H. Li, L. L. Xu, W. Wei, Z. Li, *Adv. Funct. Mater.* **2019**, *29*, 1808640.

[36] L. Jing, H. L. Li, R. Y. Tay, B. Sun, S. H. Tsang, O. Cometto, J. J. Lin, E. H. T. Teo, A. I. Y. Tok, *ACS Nano* **2017**, *11*, 3742.

[37] a) J. J. Tian, H. Q. Feng, L. Yan, M. Yu, H. Ouyang, H. Li, W. Jiang, Y. M. Jin, G. Zhu, Z. Li, Z. L. Wang, *Nano Energy* **2017**, *36*, 241; b) G. M. Wang, H. Q. Feng, L. S. Hu, W. H. Jin, Q. Hao, A. Gao, X. Peng, W. Li, K. Y. Wong, H. Y. Wang, Z. Li, P. K. Chu, *Nat. Commun.* **2018**, *9*, 2055.